

PLR (Plastic Lithium Rechargeable) Batteries using Nanoscale Materials : A Convenient Source of Electrical Energy for the Future?[†]

G. Campet,* N. Treuil, A. Poquet, S. J. Hwang, C. Labrugère,‡ A. Deshayes,§
J. C. Frison,# J. Portier, J. M. Reau, and J. H. Choy^{††}

*Institut de Chimie de la Matière Condensée de Bordeaux du CNRS, Château Brivazac,
avenue du Dr. A. Schweitzer, 33608 Pessac, France*

[‡]*Centre de Caractérisation des Matériaux Avancés, Château Brivazac, Avenue du Dr. A. Schweitzer, 33608 Pessac, France*

[§]*Centre National d'Etudes des Télécommunications, 38-40 rue du Général-Leclerc, 92131 Issy-les Moulineaux, France*

[#]*Centre National d'Etudes des Télécommunications, 2 route de Trégastel, BP 40, 2301 Lanion, France*

^{††}*Department of Chemistry, Center for Molecular Catalysis, Seoul National University, Seoul 151-742, Korea*

Received March 27, 1999

This communication describes the synthesis of : (i) non-toxic and low cost nanocrystalline electrode materials, which can be prepared advantageously at low temperature ; (ii) highly conductive electrolyte membranes formed by the nano-encapsulation within a poly(acrylonitrile)-based polymer matrix of a solution of LiPF₆ in organic solvents. The performances of rechargeable PLR (Plastic Lithium Rechargeable) batteries using the above mentioned components are presented.

Introduction

Two phenomena call for special attention.

(1) Recent advances in portable electronic devices (portable computers, cellular phones, camcorders, etc.) have resulted in significant demand for miniaturized power sources to power these systems.

(2) Mankind is becoming increasingly aware of the damage to health and the environment cause a by the release of noxious gases into the atmosphere. Since most of these toxic emissions come from fossil fuel burning vehicles, especially in big cities, high-energy, rechargeable power sources are needed for the development of long-range electric vehicles, which would lead to an improvement in air quality.¹

These two demands have motivated research on electrical energy systems that will be more powerful and take up less space than conventional batteries. Obviously, these new power sources must be non-polluting and non-toxic. Extensive research is in progress in the United States, Asia and Europe, and three battery systems have emerged as the most efficient for electric transportation application.¹⁻⁵ As reported by Megahed, S. and Scrorati, B.,¹ the first system uses a molten sodium anode, a sulfur-impregnated carbon felt cathode and a solid sodium ion-conducting electrolyte ; the second one uses a Li-Al anode, an iron disulfide cathode, and a molten LiCl-LiBr-KBr electrolyte. However, these two systems operate at high temperature (above 300 °C)¹ and are therefore inappropriate for portable electronic devices. That is not the case for the third nonaqueous systems, the so-called lithium batteries, which can be used efficiently at room temperature and are therefore being

intensively studied. They are based on a lithium metal or a lithium-inserted graphite as anode, a lithium-ion conducting electrolyte and a cathode material. The cathode material must be both an ionic and electronic conductor having generally an open structure (layered or tunneled), enabling the reversible intercalation of lithium ions. Among the most efficient cathode materials are transition metal dichalcogenides or oxides such as TiS₂, LiNiO₂, LiCoO₂, LiMn₂O₄, and V₆O₁₃.⁶⁻³⁰

For the sake of clarity, the working principle of such a Li battery is illustrated in Figure 1. In Table 1, the efficiencies at room temperature of Li batteries are compared with those of the more conventional systems of Ni-Cd (nickel-cadmium) and Ni-MH (nickel-metal hydride). A lithium battery having a weight of 225 kg can power an electric car for 200 km at a speed of 120 km/h. For the same vehicle, the performance is much lower for the Ni-MH battery and obviously even lower for the Ni-Cd battery.

Consequently, it appears that *lithium batteries* represent (together with *fuel cells*,³¹ which are not the subject of this

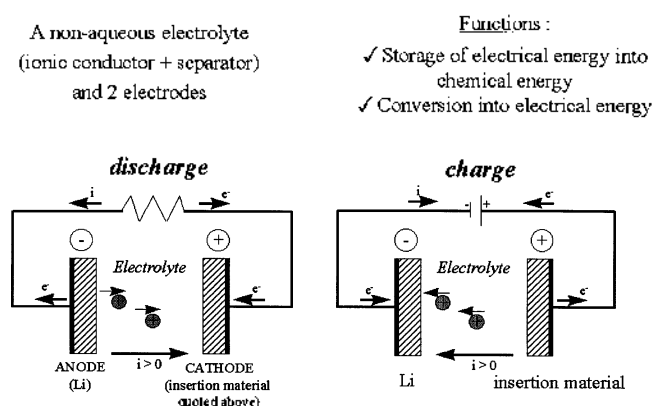


Figure 1. Principle of the rechargeable lithium battery.

[†]Basis of the presentation given at International Joint Seminar on New Trends in Material Chemistry 12-13 March 1999, Seoul National University, Seoul, Korea

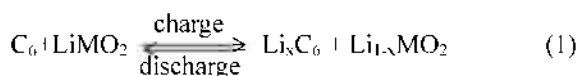
Table 1. Performance characteristics (the three main SAFT technologies, from Internet)

Parameters	Ni-Cd	Ni-MH	Li-Ion
Weight (kg)	280	260	225
Specific Energy (Wh/kg)	55	70	150
Electric Range (km)	100	130	200
Vehicle Maximum speed (km/h)	95	110	120

communication) a leap forward in energy density compared with the conventional systems.³² Nevertheless, further enhancement of the performances of electric vehicles is needed, necessitating the production of more powerful batteries that are lighter and occupy less space than existing ones. Moreover, further miniaturization of portable electronics requires a substantial reduction in the weight and size of the lithium batteries.

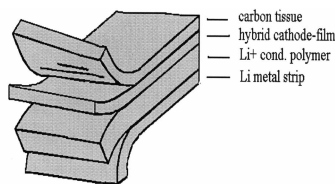
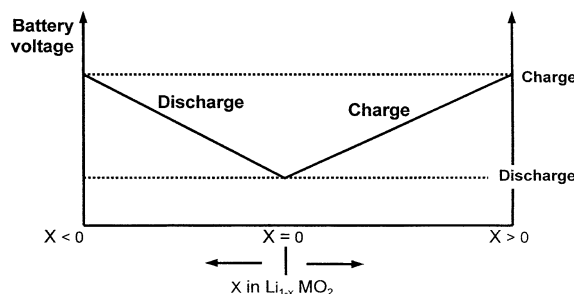
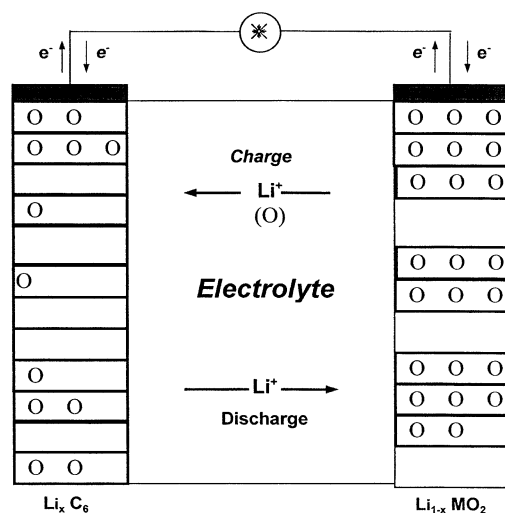
From these two points of view, we argue here that the *thin and flexible lithium batteries, the so-called PLR (Plastic Lithium Rechargeable) batteries*, are likely to fulfill the needs of both the electronic device and electric transportation markets. In the latter case, one can use the well-known roll-coating technology to achieve powerful PLR systems that occupy a smaller volume. On the other hand, in the case of the electronic market, it is apparent that PLR batteries will be able to fit the shape of the increasingly miniaturized electronic systems and even be integrated within them.¹

A PLR battery can be formed by contacting a lithium metal strip, a lithium ion conducting polymeric membrane and a composite cathode membrane obtained by blending an active lithium intercalation material with carbon and a polymer binder (Figure 2). The Li⁺ conducting polymer electrolyte membrane is obviously a key component of the battery, since the lithium metal is indeed corroded by almost any electrolyte medium. Clearly, the instability of the lithium metal/electrolyte interface is the critical problem that remains to be successfully addressed in lithium batteries and therefore in PLR systems. One way to overcome this problem is to replace the metal with carbon-type (coke or graphite) insertion compounds.^{1,33} The overall process of such batteries, so-called lithium ion batteries, is illustrated in Figure 3 and can be expressed as:^{1,33}



In fact, the use of Li_xC₆ as the lithium source instead of Li metal induces losses in specific energy; moreover, voltage

- Can be fabricated in any shape and size
- Very attractive for
 - the electric vehicle
 - the electronic consumer market
 -

**Figure 2.** The PLR battery.**Figure 3.** The lithium ion battery.

fluctuations, which can expand up to 1.5 V, can occur on cycling.^{34,35} In addition, a significant excess of cathode material is often required in order to obtain an acceptable cycle life of the lithium ion batteries, due to the irreversible capacity in the first cycle.¹ For these reasons we have targeted our research at PLR systems that involve a lithium metal film as anode with the objective of reducing: (i) the instability of the lithium metal/electrolyte interface; (ii) the probability of short-circuit, which may occur during the charging process due to the dendritic growth of lithium metal on the anode. We believed that these two problems can be circumvented with the appropriate selection and ratio of the components forming the polymeric electrolyte-membrane. If the polymeric electrolyte membrane is one of the two key components of the PLR system, the second one is obviously the electrode material. We will show here also that nanocrystalline compounds are promising electrode materials for PLR systems.

Choice of the Materials - Experimental - Discussion

Choice, Preparation and Properties of the Polymeric Electrolyte Membrane

Choice of the materials. First of all, let us state that, for obvious reasons, the polymeric electrolyte membrane must have a room temperature conductivity as close as possible to that of the liquid lithium electrolytes so that the PLR battery will be able to operate efficiently at room temperature. Classical examples of polymer electrolyte membranes include

complexes between lithium salts (e.g. LiClO_4 , LiPF_6 , etc.) and high molecular weight polymers containing Li^+ coordinating atoms (e.g. poly(ethylene oxide), PEO), where oxygen is acting as the coordinating atom.^{36,37} The main problem with PLR batteries using such polymer electrolyte membranes is their inability to operate efficiently at ambient temperature due to the very low room-temperature conductivity ($\leq 10^{-6} \Omega^{-1} \text{cm}^{-1}$) of the PEO-based electrolytes. Consequently, considerable research has been carried out to improve the room temperature performances, notably in the ACEP collaboration between Hydro-Quebec in Canada, Elf and CNRS-Grenoble in France.^{38,39} The most successful results so far have been obtained by trapping liquid electrolyte solutions in polymer cages.⁴⁰ Two distinct methods have been reported: (i) loading the liquid electrolyte into a microporous polymer; (ii) enhancing the viscosity of the liquid electrolyte by adding a soluble (in the electrolyte) polymer until a gel is achieved, which can be easily spread onto Teflon moulds leading to polymeric membranes after cooling to room temperature. The most efficient polymer additives for yielding electrolyte-membranes with the required electrical and mechanical properties are poly(methyl methacrylate) (PMMA), poly(vinylidene) fluoride with hexafluoropropylene (PVDF-HFP), and poly(acrylonitrile) (PAN).⁴¹⁻⁴⁷ We followed the above-mentioned

approach (ii) to prevent the short-circuit events, which may occur during the charging processes of the battery. We selected PAN because apparently it is the most stable versus oxidation and, as thus, will not decompose during the charging processes of the PLR batteries.⁴⁸ In addition, the PAN has polar CN groups that can interact with the liquid electrolyte, inhibiting its loss. The liquid electrolyte consists of lithium hexafluorophosphate (LiPF_6) dissolved in an appropriate mixture of ethylene carbonate (EC) and propylene carbonate (PC). The polymer-electrolyte interaction would be ensured by the labile hydrogen of PC and the polar CN groups of PAN (Figure 4). Furthermore, the solvents EC and PC have a high dielectric constant ($\epsilon_r \approx 60$), ensuring an efficient separation of the Li^+ cations from the PF_6^- anions and leading to a high room-temperature conductivity. Finally, these solvents have a low volatility so they facilitate manufacturing of the membrane with an accurate control of the ratio EC/PC.

When we started our research on PLR systems five years ago,⁴⁸ no one, to our knowledge, had used LiPF_6 in conjunction with PAN-PC-EC. The other used mainly LiClO_4 and LiAsF_6 instead of LiPF_6 because the ClO_4^- and AsF_6^- anions are less easily oxidized than PF_6^- ; therefore, the anodic stability of the electrolytes using LiClO_4 or LiAsF_6 would be greater. We observed, however, that the oxidation potential of PF_6^- remained rather high around 4.3 V vs Li.⁴⁸ In fact, in this work, we did not consider LiClO_4 due to its explosive character in the presence of organic solvents, nor did we consider LiAsF_6 due to the toxicity of arsenic. The highest cathodic stability was observed for the electrolyte membranes using LiPF_6 .⁴⁸

Manufacturing process. The manufacturing process of the polymeric electrolyte membrane is illustrated in Figure 5. The reagents were first mixed at the required mass ratio in the inert atmosphere of a dry box and then heated at 110 °C to obtain a solution of appropriate viscosity that could be easily cast onto the substrate. Membranes having a translucent elastomeric appearance were finally obtained after cool-

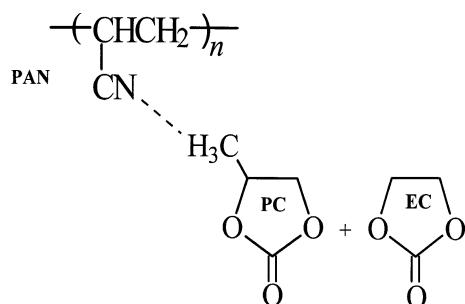


Figure 4. Structures of PAN-PC-EC showing the main polymer-solvent interaction.

① dissolution of $\text{LiPF}_6 + \text{EC} + \text{PC}$ at 25°C; drying PAN at 60 °C (48 hr.) under vacuum

② $\text{LiPF}_6 + \text{EC} + \text{PC} \xrightarrow{T^\circ \rightarrow 110 \text{ }^\circ\text{C} (20')}$ ③ dissolution of $\text{LiPF}_6 + \text{EC} + \text{PC} + \text{PAN}^*$

* An (still confidential) additive A is added to further enhance the stability of the electrolyte membrane/Li metal foil interface in the PLR systems.

④ casting of the viscous solution

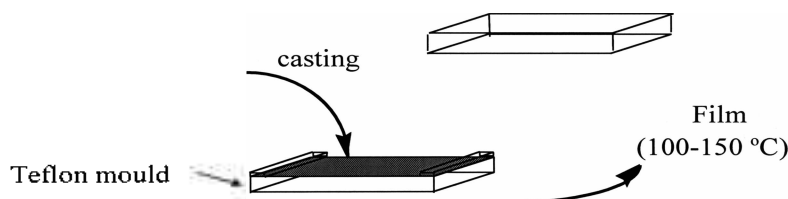


Figure 5. Manufacturing process of the electrolyte membrane.

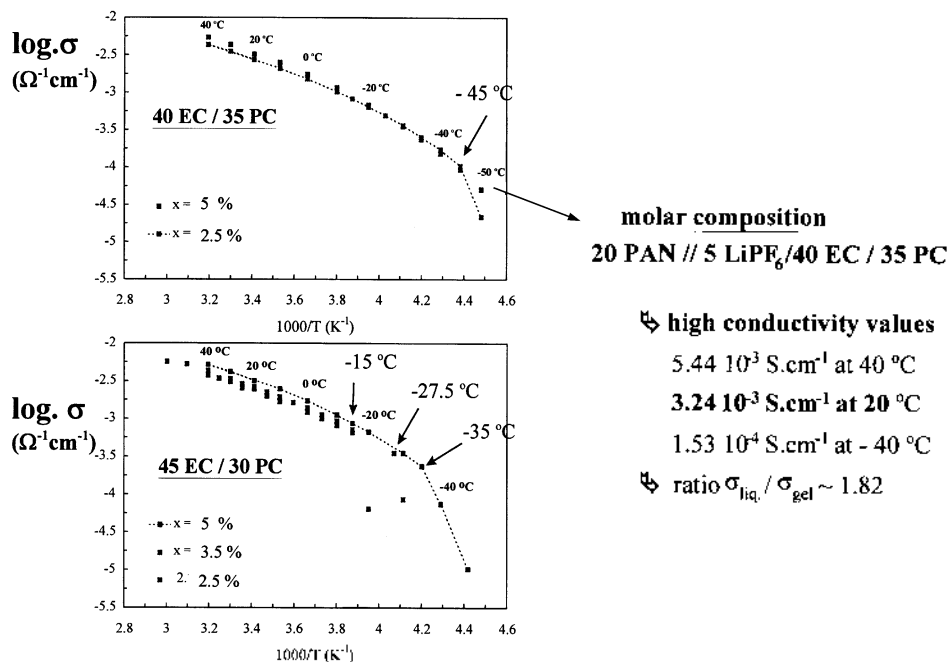


Figure 6. Ionic conductivities (Ac measurements) of hybrid electrolyte membranes of composition (molar %): 20PAN//5LiPF₆/75(EC-PC).

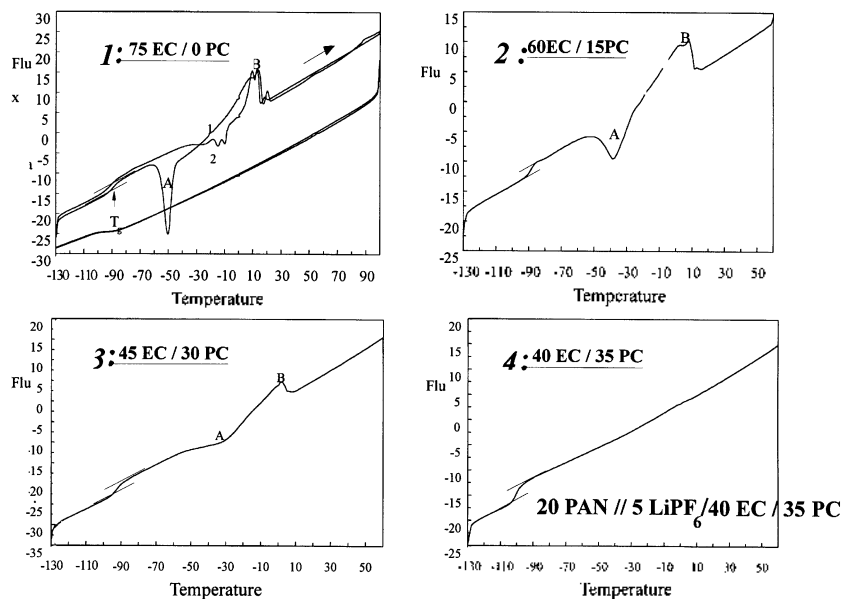


Figure 7. DSC thermograms of hybrid electrolyte membranes of composition (molar %): 20PAN//5LiPF₆/75(EC+PC).

ing at room temperature.

Main characteristics. One can easily guess that the conductivities of these hybrid electrolytes can be tailored by a judicious selection of the ratio of the different components. Among the numerous compositions that were studied,⁴⁸ we have established that the highest conductivity is achieved for the composition (molar %): 20 PAN // 5 LiPF₆ / 40 EC / 35 PC. The conductivity is indeed close to that of liquid electrolytes (Figure 6).⁴⁸ Also, the membrane has the required dimensional stability, with a Young modulus of ~1.7 MPa at 25 °C.⁴⁸ Figure 6 shows that this composition is rather critical: a slight modification of the EC/PC ratio or of the LiPF₆ content induces a drop in conductivity, particularly at

low temperature. In fact, this drop in the conductivity arises from a crystallization process. The latter is illustrated in Figure 7, which shows the DSC thermograms of various membranes having different proportions of EC and PC. The peaks A and B, which appear only for membranes 1, 2 and 3, account for a crystallization process (peak A) followed by a melting process of the crystallized species (peak B). It is noteworthy that membrane 4, which does not undergo any visible crystallization process (Figure 7), has the highest conductivity (Figure 6). It corresponds to the composition (molar %): 20 PAN // 5 LiPF₆ / 40 EC / 35 PC. In fact, the drop in conductivity observed for the other compositions (Figure 6) which exhibit the crystallization process evi-

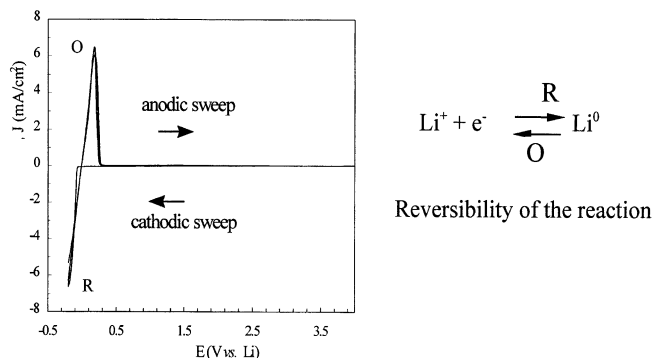


Figure 8. Potential sweep, J (F), of a stainless steel electrode vs Li metal foil sandwiching the membrane* 4 (see Figure 7) having the highest conductivity (see Figure 6). *the additive A (see Figure 5) is added.

denced in Figure 7, would imply that the crystallized species involve Li^+ ions trapped in crystallized EC. On the other hand, for membrane 4 (Figure 7) having the highest conductivity, all EC interact efficiently with PC so that no crystallization of EC occurs. Figure 8 illustrates the rather good electrochemical stability of membrane 4. The electrochemical stability window was determined by running voltammetry sweeps of a stainless steel blocking electrode vs a lithium-foil counter-electrode.

The results imply that membrane 4 could be used advantageously as electrolyte for efficient PLR systems.

Choice, Preparation and Properties of the Cathode Materials

Choice of the materials. Commercially available lithium batteries use layered LiCoO_2 cathodes.⁴⁹ But the high cost and toxicity of cobalt gave impetus to the development of cheaper, non-toxic electrode materials. From this prospective, nanocrystalline and/or X-ray amorphous lithium-manganese oxides are very attractive alternatives;⁵⁰⁻⁵³ what's more, these materials can be easily prepared at low temperature, leading to low-cost manufacturing processes. Ten years ago, we showed, using many examples, that the control of crystallite size is a key factor in determining the electrochemical performances of the electrodes. The following "electrochemical model" was deduced:⁵¹ Nanocrystalline materials are likely to have an enhanced electrochemical activity, compared with that of their microcrystalline homologues, provided that the first electrochemical process that intervenes is a discharge of the Li battery. The discharge should begin with an electrochemical grafting of the Li^+ ions at/near the crystallite surface. The structural defects or distortions at/near the crystallites, which are more obvious in the nanoscale region than in the microscale region, can indeed act as reversible grafting sites for Li^+ ions. The following second electrochemical step occurs during the discharge of the Li battery (when the crystallite structure is adapted): intercalation of the Li^+ ions into the crystallites. In this case, the discharge-charge electrochemical process can be depicted as: grafting \rightarrow intercalation \rightarrow deintercalation \rightarrow degrafting. These concepts are important because they allow us to foresee when it is preferable to use nanocrystal-

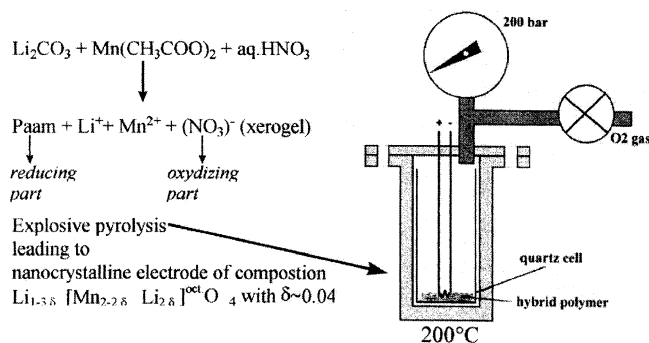


Figure 9. Manufacturing process of the nanocrystalline LiMn_2O_4 electrodes.

line electrode materials (or microcrystalline electrode materials), depending on whether the first electrochemical process of the Li battery is a discharge (or a charge).

We illustrate here these concepts for two different nanocrystalline electrode materials based on lithium manganese oxide:

- (i) nanocrystalline spinel-type " LiMn_2O_4 "^{48,52}
- (ii) nanocrystalline rock-salt type " Li_2MnO_3 "^{50,48}

Synthesis process

- (i) The nanocrystalline spinel electrode prepared at 200 °C

An original polymeric route which we have recently patented⁵³ has been used, as depicted in Figure 9. Homogeneous starting materials were obtained from an aqueous HNO_3 (1N) solution to which appropriate amounts of polyacrylamide (PAam, Aldrich M.W. = 10,000), lithium carbonate (Aldrich 99.997%) and manganese (II) acetate tetrahydrate (Aldrich 99+%) were added. First, a gel is formed and a xerogel (hybrid polymer) is prepared after removal of the solvent. The controlled explosive oxo-reduction reaction – occurring at ~ 200 °C under oxygen atmosphere (Figure 9) – of the hybrid polymer leads to ultrafine crystallites (~ 50 Å) of the spinel phase of composition

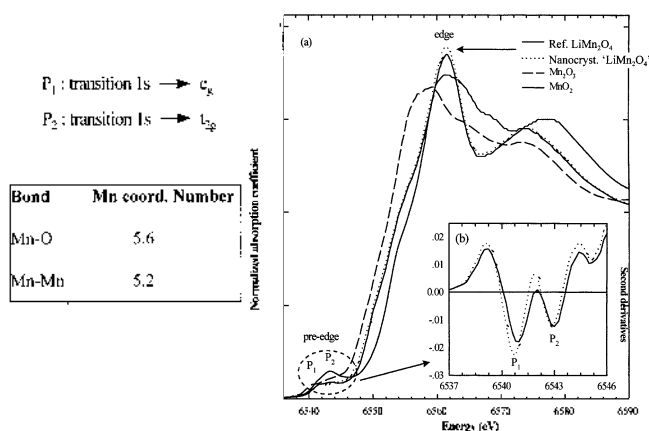


Figure 10. MnK-edge KANES spectra for the nano crystalline " LiMn_2O_4 " and the references. The average oxidation state of Mn, which is higher than 3.5, and the Mn-O, Mn-Mn coordination numbers, which are lower than 6, observed for the nanocrystalline " LiMn_2O_4 " have been deduced from XAS analysis. They were correlated to the higher structural disorder which is characteristic of the nanocrystalline texture.⁵²

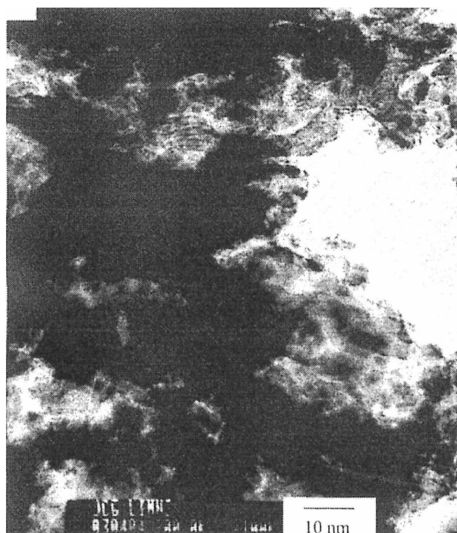


Figure 11. TEM micrograph of nanocrystalline LiMn_2O_4 . The average crystallite size is $\sim 50 \text{ \AA}$.

$\text{Li}_{1.5\delta}\text{Li}_{3\delta}[\text{Mn}^{1.3,552}_{2.2\delta}\text{Li}_{2\delta}]^{0\delta}\text{O}_4$ with $\delta \equiv 0.02$.^{48,53} The latter was deduced from the combination of chemical titration, XPS,⁴⁸ and XAS analysis,⁵² (Figure 10). The TEM micrograph (Figure 11) and XRD pattern (Figure 12) are characteristic of the nanocrystalline texture with an average crystallite size of 50 \AA .

(ii) The nanocrystalline rock-salt type electrode prepared at room temperature

As reported by Kim, J. and Manthiram, A.,⁵⁰ complex metal oxides are usually prepared by firing the raw materials at elevated temperature. This approach cannot yield to the accessibility of metastable nanocrystalline and/or X-ray amorphous phases, which may be highly attractive as electrode materials for lithium batteries, according to ref.^{50,51,52,54} and also according to the "electrochemical model" reported above. Here we used LiI to reduce the permanganate ion ($\text{Mn}^{\text{VII}}\text{O}_4$) in Na⁺-containing aqueous medium⁵⁰ to produce a Mn^{IV}-rich nanocrystalline oxide with a composition close to Li_2MnO_3 . The detailed preparation process is illustrated in Figure 13. The as-prepared sample was found to be amorphous to X-ray diffraction, as similarly

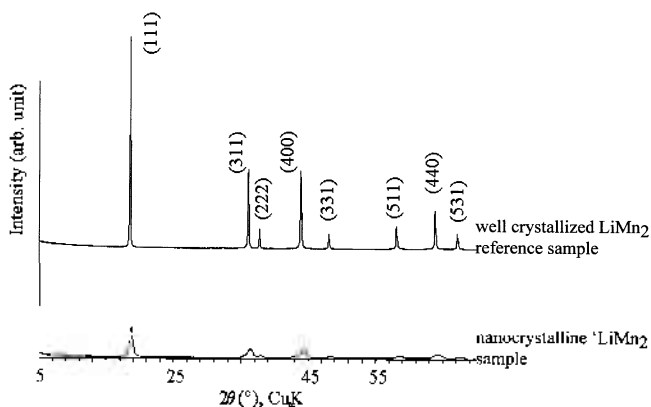


Figure 12. X-ray diffraction pattern characteristic of the nanocrystalline structure of LiMn_2O_4 .

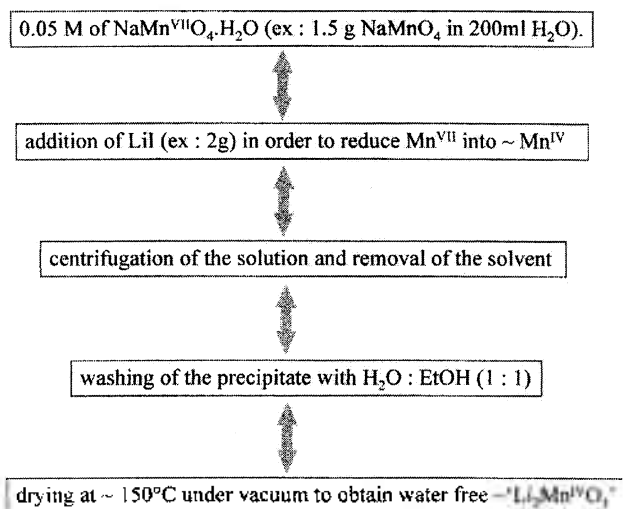


Figure 13. Synthesis process of the nanocrystalline rock-salt type $\text{Li}_2\text{Mn}^{\text{IV}}\text{O}_3$.

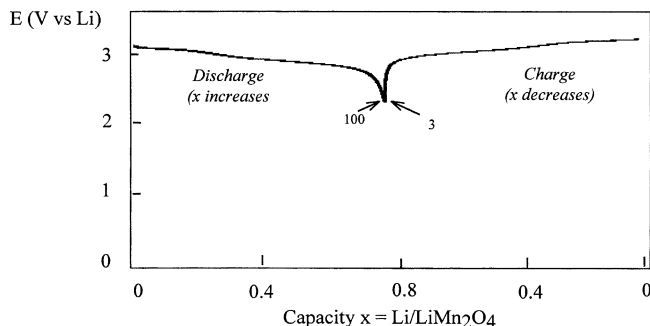


Figure 14. Discharge/charge behavior ($C/5$) with the number of cycles for the PLR cells using nanocrystalline LiMn_2O_4 .

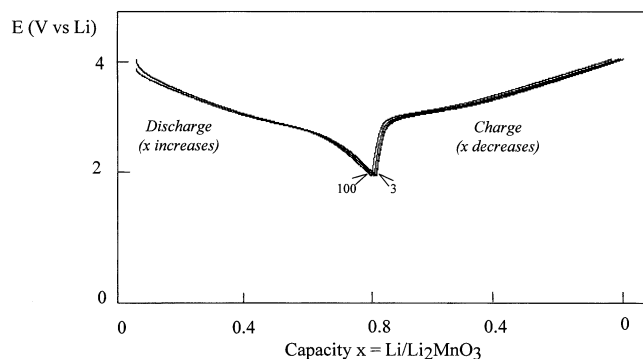


Figure 15. Discharge/charge behavior ($C/5$) with the number of cycles for the PLR cells using nanocrystalline Li_2MnO_3 .

observed by Kim, J. and Manthiram, A.. The detailed textural and structural investigation using XPS, XAS, TEM, XRD etc. is currently in progress and will be reported later.

Electrochemical Properties of the PLR Batteries

The electrochemical measurements were performed using a computer-controlled potentiostat/galvanostat (Tacussel, PGS 201T model) for the PLR cells assembled by sandwiching the polymer electrolyte (membrane 4 in Figure 7)

between the lithium anode foil and the composite cathode. The composite cathode was made according to the preparation procedure we have proposed^{48,53} and the procedure proposed by Sun, Y. K. and Jin, S. H. for their efficient PLR cells.⁵⁶ The as synthesized nanocrystalline "LiMn₂O₄" (or "Li₂MnO₃") powder was added to PAN solution in demethyl sulfoxide (DMSO) as a solvent. The slurry was spread onto a carbon active tissue of ~2000 m²/g surface area (Actitex) and dried under vacuum for 16 h at 110 °C. The dried composite cathode was then compressed with a roll-presser in the inert atmosphere of a dry box. The cells based on nanocrystalline "LiMn₂O₄" and "Li₂MnO₃" were cycled between cut-off voltages of 2.2-3.2 V_{Li/Li+} and of 2-4 V_{Li/Li+}, respectively, at a current density of 1 mA/cm² (C/5). The reversible capacity corresponds to ~ 0.8 mole of Li per mole of electrode material as shown in Figures 14 and 15. This rather high and reversible capacity was related to the presence of the structural defects arising from the nanoscale structure, in agreement with the "electrochemical model" reported above. The influence of the structural defects has been investigated recently using XAS or Li NMR⁵² and also the evolution of the open circuit voltage of the cell as a function of the inserted Li.⁴⁸

Conclusion

The PLR batteries based on the electrolyte membrane of composition (molar %) : 20 PAN // 5 LiPF₆ / 40 EC / 35 PC sandwiched between Li foil and nanocrystalline "LiMn₂O₄" or "Li₂MnO₃" composite cathode appears to be highly attractive from the industrial point of view, although further investigation is needed.

References

- Megahed, S.; Scrosati, B. *The Electrochemical Society Interface* **1995**, 35-37.
- Henriksen, G. L.; De Luca, W. H.; Vissers, D. R. *Chemtech* **1994**, 32-35.
- Cairns, E. J. *Interface* **1992**, 1, 24-26.
- Commission of the European Communities, Joule II-Programme, Energy Conservation and Utilization*, Brussels.
- Ishikawa, R.; Hazama, T.; Miyabashi, M.; Andoh, H. *Proceedings of the International Workshop on Advanced Batteries*; Osaka, Japan, 1995; pp 22-24.
- Rouxel, J. *Physica* **1980**, 99B, 3-6.
- Armand, M. *Doctoral Thesis*, Inst. National Polytech. de Grenoble, 1978.
- Delmas, C.; Fouassier, C.; Hagenmuller, P. *J. Phys. Chem. Solids* **1978**, 39, 55-61.
- Molenda, J. *Solid State Ionics* **1986**, 21, 263-269.
- Levasseur, A.; Menetrier, M. *Mat. Sci. Eng. B* **1989**, 3, 5-10.
- Takehara, Z. I.; Kanamura, K. *Electrochimica Acta* **1993**, 38, 1169-1173.
- Abraham, K. M. *Electrochimica Acta* **1993**, 38, 1233-1238.
- Broussely, M.; Pertion, F.; Labat, J.; Staniewicz, R.; Romero, A. *J. Power Sources* **1993**, 45, 209-214.
- Nagaura, T. *Proceedings of the 4th International Rechargeable Battery Seminar*; Deertfield Beach, Florida, U.S.A., 1990.
- Dahn, J. R.; Von Sacken, V.; Fong, R. *Proceedings of the 178th Meeting of the Electrochemical Society*; Seattle, Washington, U.S.A., 1990.
- Koetschau, I.; Richard, M. N.; Dahn, J. R.; Soupart, J. B.; Rousehe, J. C. *J. Electrochemical Soc.* **1995**, 142, 2906-2910.
- Progress in Batteries and Battery Materials*; Brodd, Ralph J., Ed.; ITC-JEC Press Inc, 1995; Vol. 14.
- Lithium Battery: New Materials, Development and Perspectives*; Pistoia, G., Ed.; Elsevier Science B.V.: 1994.
- Goodenough, J. B.; Thackeray, M. M.; David, W. I. F.; Bruce, P. G. *Revue de Chimie Minérale* **1984**, 21, 435-441.
- Gummow, R. J.; de Kock, A.; Thackeray, M. M. *Solid State Ionics* **1994**, 69, 59-62.
- Tarascon, J. M. *US Patent 5*, **1995**, 424, 205-209.
- Kokband, R.; Barker, J. *Solid State Ionics* **1996**, 84, 1-5.
- Ohzuku, T.; Kitawaga, M.; Hirai, T. *J. Electrochem. Soc.* **1991**, 137, 769-772.
- Tarascon, J. M.; Wang, F.; Shokoohi, F. K.; McKinnon, W. R.; Colson, S. *J. Electrochem. Soc.* **1991**, 138, 2859-2864.
- Manev, V.; Momchilov, A.; Nassalevska, A.; Sato, A. *J. Power Sources* **1995**, 54, 323-327.
- Jiang, Z.; Abraham, K. M. *J. Electrochem. Soc.* **1996**, 143, 1591-1593.
- Barboux, P.; Tarascon, J. M.; Shokoohi, F. K. *J. Solid State Chem.* **1991**, 94, 185-189.
- Huang, H.; Bruce, P. G. *J. Electrochem. Soc.* **1994**, 141, 1106.
- Liu, W.; Farrington, G. C.; Chaput, F.; Dunn, B. *J. Electrochem. Soc.* **1996**, 143, 879-882.
- Linden, D. *Handbook of Batteries*, 2nd Ed.; Wiley: New York, 1995.
- The fuel cell technology also offers a solution to the problem of the damaging health and environmental effects of releasing noxious gases into the atmosphere in the form of a clean and zero-emission option for both the transportation and power generation industries (see for instance the article of Mike Lain from AEA technology in UK: "Membrane fuel cells provide a breath of fresh air": Membrane Technology No.87).
- Bruce, P. G. *Philos. Trans. R. Soc. London, Ser. A*. **1996**, 354, 1577-1580.
- Scrosati, B. *J. Electrochem. Soc.* **1992**, 139, 2276-2280.
- Tarascon, J. M.; Guyomard, D. *J. Electrochem. Soc.* **1992**, 139, 937-941.
- Passerini, S.; Rosolen, M.; Scrosati, B. *J. Power Sources* **1993**, 45, 333-338.
- Armand, M. B.; Chabagno, J. M.; Duclot, M. *2nd Int. Meet. Solid Electrolytes*; St. Andrews, Scotland, U.K., 1978.
- Gray, F. M. *Solid Polymer Electrolytes*; VCH: New York, 1991.
- Gauthier, M.; Fauteux, D.; Vassort, G.; Belanger, A.; Duval, M.; Rieoux, P.; Chabagno, J. M.; Muller, D.; Rigaud, P.; Armand, M.; Peroc, D. *J. Electrochem. Soc.* **1985**, 132, 1333-1340.

39. Armand, M.; Gorecki, W.; Andreani, R. *Proc. 2nd Int. Symp. Polymer Electrolytes*, Siena, Italy, Ext. Abstr, 1989.
 40. Croce, F.; Brown, S. D.; Greenbaum, S. G.; Slane, S. M.; Salom, M. *Chem. Mater.* **1993**, *5*, 1268-1272.
 41. Bohmke, O.; Rousselot, C.; Gillet, P. A.; Truche, C. *J. Electrochem. Soc.* **1992**, *139*, 1862-1865.
 42. Watanabe, M.; Karba, M.; Nagaoka, K.; Shinohara, I. *J. Polym. Sci., Polym. Phys. Ed.* **1983**, *21*, 939-945.
 43. Abraham, K. H.; Alamgir, M. *J. Electrochem. Soc.* **1990**, *106*, 1657-1660.
 44. Schmutz, C.; Tarascon, J. M.; Gozdz, A. S.; Warren, P. C.; Shokoohi, F. K. *Rechargeable Lithium and Lithium-Ion Batteries*, Megahed, S., Barnett, B. M. and Xie, L., **1994**, PV 94-28, pp. 330-333. The Electrochemical Society Proceedings Series, Pennington, N. J., 1994; pp 330-333.
 45. Alamgir, M.; Abraham, K. M. *J. Power Sources* **1995**, *54*, 40-44.
 46. Rosanski, H. G.; Irving, I. D. *Electronic Engineering Times*, May 23, 1994.
 47. Tarascon, J. M.; Gozdz, A. S.; Schmutz, C.; Shokoohi, F.; Warren, P. C. *Solid State Ionics* **1996**, *86-88*, 49-54.
 48. Treuil, N. *Ph. D. Thesis*, Univ. Bordeaux I, 1998.
 49. Nagura, T.; Tozawa, K. *Prog. Batteries Sol. Cells* **1990**, *9*, 209-1217.
 50. Kim, J.; Manthiram, A. *Nature* **1997**, *390*, 265-267.
 51. Campet, G.; Treuil, N.; Deshayes, A.; Frison, J. C.; Portier, J.; Rabardel, I. *Active and Passive Elec. Comp.* **1998**, *21*, 167-181, and references therein.
 52. Treuil, N.; Labrugère, C.; Menetrier, M.; Portier, J.; Campet, G.; Deshayes, A.; Frison, J. C.; Hwang, S. J.; Song, S. W.; Choy, J. H. *J. Phys. Chem. B* **1999**, *103*, 2100.
 53. Treuil, N.; Portier, J.; Campet, G.; Frison, J. C. *CNET patent n°9612690*, 1996.
 54. Stein, A.; Keller, S. W.; Malbouk, T. E. *Science* **1993**, *259*, 1558-1564.
 55. Sun, Y. K.; Jin, S. H. *J. Mater. Chem.* **1998**, *8*, 2399-2404.
-